

Gametogenesis, embryogenesis, and larval features of the oviparous sponge *Petrosia ficiformis* (Haplosclerida, Demospongiae)

Manuel Maldonado · Ana Riesgo

Received: 29 January 2009 / Accepted: 18 June 2009 / Published online: 8 July 2009
© Springer-Verlag 2009

Abstract This study describes the reproductive cycle of *Petrosia ficiformis* and documents for the first time embryogenesis in an oviparous haplosclerid demosponge. Gonochoric adults, occurring in 2:1 female/male ratios, spawned in late autumn, after a 7-month long oogenesis and a 2.5-week-long spermatogenesis. Following a remarkable migration, the oocytes were released as 250 µm eggs bearing attached polar bodies and a thin mucous cover. Round-headed spermatozoa with three large mitochondria, and many proacrosomal vesicles fertilized the eggs externally. A fertilization membrane appeared around the zygotes. Nearly equal and total cleavage led to a stereoblastula that subsequently became an entirely ciliated larva. The larva alternated spherical and multilobate body shape and consisted of undifferentiated cells. It had poor abilities to swim and glide, probably experiencing passive dispersal and unselective attachment. Settlers developed choanocyte chambers after 1.5 months. Symbiotic microbes were absent from gametes and larvae, being necessarily acquired from the ambient at each sponge generation.

Introduction

The haplosclerid demosponge *Petrosia ficiformis* (Poiret 1789) is one of the most prominent members in Mediterranean sublittoral rocky communities. It ranks among the largest organisms, with a red-wine colored, massive-lobate body that operates as a microhabitat itself, hosting diverse invertebrates (ophiuroids, shrimps, polychaetes, cnidarians, mollusks, etc). In addition, the massive silica skeleton of this sponge has been suggested to act as a substantial trap for silicate, a relevant nutrient also required for primary production (Maldonado et al. 2005). The sponge is also the source of several bioactive metabolites (e.g., Ferretti et al. 2007) and hosts a diverse community of both phototrophic and heterotrophic microbes that are diversely integrated in the host metabolism (e.g., Regoli et al. 2004).

Sets of unpublished observations suggest that *P. ficiformis* may follow a “K” ecological strategy, with very low growth and recruitment rates so that its population may require some conservationist attention in the highly impacted Mediterranean sublittoral (Barea-Azcón et al. 2008). For instance, after nearly 20 years of repetitive diving on local Mediterranean rocky-bottom communities (northwestern Spanish coast), we have observed neither noticeable recruitment nor individual growth of *P. ficiformis*. Such a perception fully agrees with the results of an unpublished photographic 10-year monitoring (Teixidó and Garrabou, pers. comm.) of 28 individuals, which revealed no appreciable individual growth during the study. Likewise, recruitment was not detected, while mortality reached 7%. Death of some large individuals by unidentified infectious agents has also been noticed by other authors (Cerrano et al. 2001; authors, unpublished observations). These data suggest that if the populations of *P. ficiformis* are anyhow damaged, they will require very long periods

Communicated by M. Byrne.

Electronic supplementary material The online version of this article (doi:10.1007/s00227-009-1248-4) contains supplementary material, which is available to authorized users.

M. Maldonado (✉) · A. Riesgo
Department of Aquatic Ecology, Centro de Estudios Avanzados de Blanes (CSIC), Acceso Cala St. Francesc 14,
Blanes, 17300 Girona, Spain
e-mail: maldonado@ceab.csic.es

(decades) for eventual recovery. If we were urged to carried out conservation actions, the current shortage of information on the life cycle and reproductive biology of this emblematic organism would put at risk the chances of success.

Taxonomically, the genus *Petrosia* belongs to the family Petrosiidae in the order Haplosclerida. Most members of this order are hermaphrodites that undergo internal fertilization, brood their embryos (viviparism) and release a free-swimming parenchymella larva. Nevertheless, three haplosclerid families—taxonomically distinguished as the suborder Petrosina (i.e., Petrosiidae, Phloeodictyiidae, Calcifibrospongidae)—are long suspected to be oviparous (i.e., gonochoric broadcasters). The available reproductive information on the suborder Petrosina is notably scarce, derived mostly from observations on the petrosiid genus *Xestospongia*. Males and females of several species of *Xestospongia* have occasionally been observed to release their gametes synchronously for external fertilization (Fromont and Bergquist 1994; Ritson-Williams et al. 2005). Such observations have fostered the idea that this should also be the case for the entire suborder Petrosina. Because externally fertilized eggs collected after a field spawning of *Xestospongia bergquistia* divided and differentiated into small, larval-like, ciliated embryos after 4 days (Fromont and Bergquist 1994), it had also been assumed that all Petrosina disperse through a parenchymella-like, free-swimming larval stage, as their viviparous haplosclerid counterparts do (see reviews by Maldonado and Bergquist 2002; Maldonado 2006). However, this view is now challenged because recent molecular studies based on the rRNA (Redmond et al. 2007; Redmond and McCormack 2008) strongly suggest that both the family Petrosiidae and the suborder Petrosina may be polyphyletic: the viviparous genera *Petrosia* and *Xestospongia* being placed in different subclades of the order Haplosclerida.

To our knowledge, the only available information on the sexual cycle of *P. ficiformis* derives from a light microscopy study based on the sections of 1,602 individuals (Scalera-Liaci et al. 1973). The study revealed this species to be gonochoric, but with a vast majority (67.8%) of individuals not producing gametes at the time of reproduction. More importantly, individuals having oocytes (31.7%) largely outnumbered individuals bearing spermatid cysts (0.5%). It was unresolved whether the low number of individuals (32.2%) involved in sexual reproduction and the overwhelming female (64:1) overabundance were part of a peculiar reproductive strategy or the result of difficulties to identify male individuals. The oogenesis of *P. ficiformis* has partially been described (Lepore et al. 1995), but the spermatogenesis and the spermatozoon are yet to be documented by TEM. There is

no information on gamete release, embryogenesis, and the larval stage.

Here, we present new information on the process of gametogenesis, fertilization, and embryogenesis of *P. ficiformis*. This information is improving our knowledge of the reproductive biology and the life cycle of this organism, and it also expected to foster further studies for a better phylogenetic understanding of the biological heterogeneity in the current order Haplosclerida.

Materials and methods

Dynamics of gametogenesis

Populations of *Petrosia ficiformis* typically consist of sparsely scattered individuals, growing preferentially at semi-shaded rocky walls and overhangs. We investigated a population established at rocky cliffs (7–16 m deep) in the Spanish Mediterranean coast between Blanes (40°40'20" N; 2°48'13" E) and Tossa de Mar (41°42'53" N; 2°56'05" E).

To investigate reproductive activity in the population over annual cycles, we tagged 5 large, presumably mature individuals and sampled their tissue monthly for gamete occurrence from October 2003 to December 2005. Samples consisted of approximately 1 × 0.5 × 0.5 cm tissue pieces collected by scuba diving using surgical scissors. Although wounds caused by our sampling healed very slowly (2–3 months; Fig. 1a) compared with other species (a few days) in no case did repetitive tissue collection cause death. When sampling of tagged individuals revealed that gametogenetic activity was about to peak in the population, which happened in autumn, we increased both sampling frequency (10-day intervals) and the number sampled individuals, which ranged from 7 to 19, depending on year and specimen abundance in the diving area.

Tissue samples were maintained in ambient seawater for transportation to the laboratory (1 to 2 h). For optical microscopy, samples were fixed, dehydrated, embedded, stained, and studied as detailed elsewhere (Riesgo et al. 2007; Maldonado and Riesgo 2008a). To estimate densities of gametes over time, we took three pictures (100×) of each of two non-serial sections per individual, following the protocol detailed elsewhere (Maldonado and Riesgo 2008a). Digital histological images were used to measure or count gametes and study histological features. We estimated the number of oocytes per mm³ (O) of tissue in female sponges over time by applying the following equation,

$$O = (N(t/(d + t))F$$

where N is the number of oocytes counted in the 7 mm² field of the histological sections, t is thickness of section (5 μm), d is average diameter of oocytes for each month,

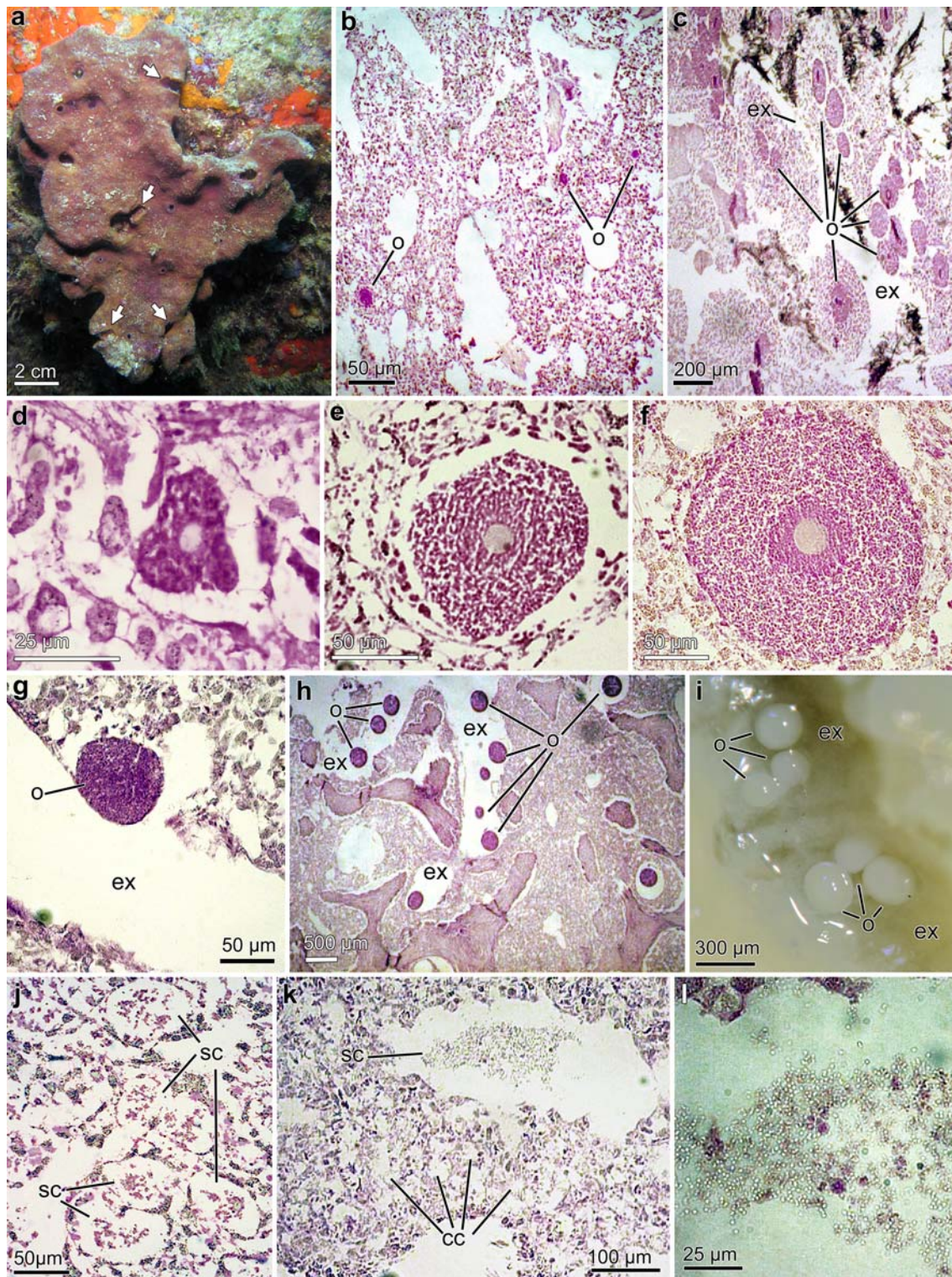
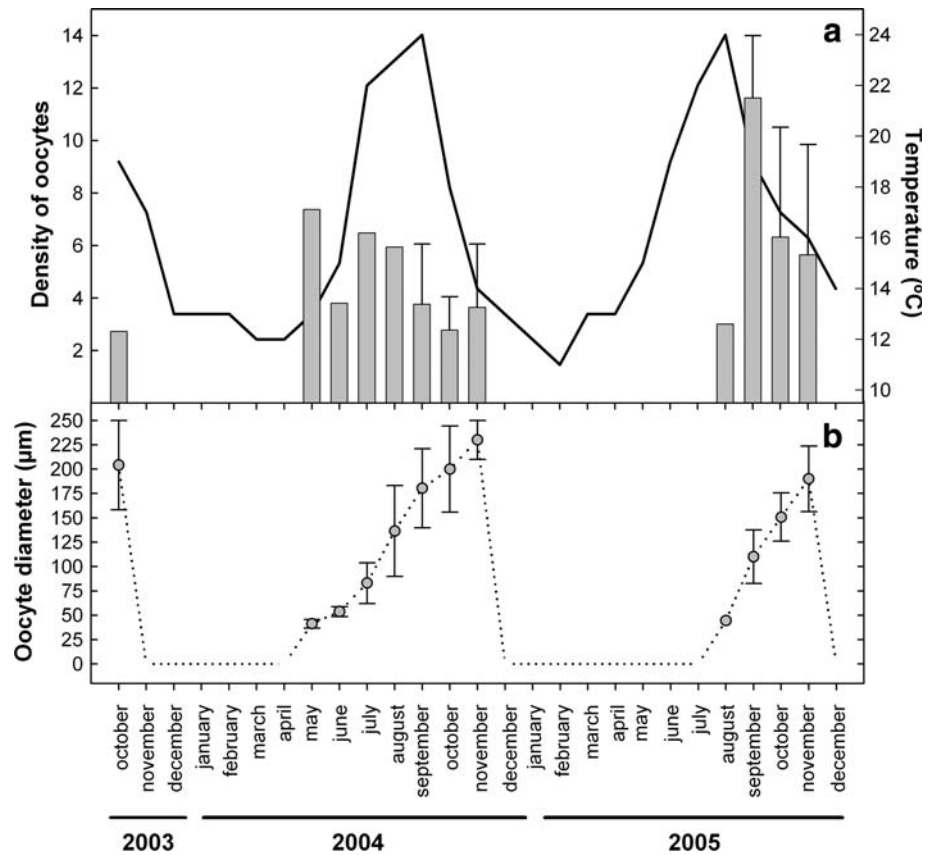


Fig. 1 **a** Large male of *P. ficiformis* at 12 m depth. Note the scars (arrows) produced by our periodical tissue sampling. **b** Early oocytes (*o*) scattered in the deep mesohyl, as visualized using light microscopy. **c** Late oocytes (*o*) aggregated in the vicinity of excurrent canals (*ex*). **d–f** Comparative size and shape of oocytes in early, mid, and late stages, respectively. **g** Late oocyte (*o*) breaking through the

epithelium of an excurrent canal (*ex*). **h–i** Oocytes (*o*) after migration to the excurrent canals (*ex*) for imminent spawning. **j–k** Early and late stages of spermatogenic cysts (*sc*), which are far larger than choanocyte chambers (*cc*), as viewed through light microscopy. **l** Detail of a nearly mature spermatogenic cyst, showing the heads of the spermatozoa clumped in the center of the lumen

Fig. 2 a Seawater temperature during two annual cycles and its relationship with mean (\pm SD) oocyte density (number of oocytes per cm^3 of mesohyl) in *P. ficiformis*. **b** Oocyte size (mean \pm SD) over two annual cycles



and $F (=28.5)$ is a factor converting the volume of observation to 1 mm^3 (Elvin 1976; Maldonado and Riesgo 2008a). Because of serious difficulties in detecting early spermatid cysts by light microscopy during 2004 and 2005, we did not quantify them over time, but instead recorded their presence/absence in the individuals during 2006 and 2007s samplings to refine sex ratio estimations. The potential relationship between oogenetic activity and seawater temperature was examined by plotting monthly estimates of oocyte density versus monthly temperature. Temperature averages derived from measurements during 3 to 5 dives a month at the local habitat using a Suntoo underwater thermometer ($\pm 0.5^\circ\text{C}$).

Ultrastructure of gametes

Transmission electron microscopy (TEM) was used when needed to describe the ultrastructure of developing and spawned gametes. Tissue samples for TEM observation were prepared and studied following the protocol detailed elsewhere (Riesgo et al. 2007; Maldonado and Riesgo 2008a).

Embryos and larvae

Based on the information on gametogenesis dynamics obtained during the 2003–2005 sampling, we predicted

spawning in 2006 and 2007. To complete the qualitative information on sexual condition (female, male, or non-reproductive), gamete release, and fertilization, we tagged 26 individuals and monitored them every 3 days during the weeks at which spawning was expected. Upon release, gametes were collected by scuba using 60 ml plastic syringes and mixed in the laboratory for fertilization. Resulting embryos, larvae, and juveniles were cultured in Petri dishes filled with unfiltered seawater in a temperature-controlled (16°C) room for 3 months and monitored periodically. In vivo observations were made under both dissecting and compound microscopes connected to a digital camera and a digital time-lapse video recorded. At different steps of the development process, embryos were also fixed for TEM.

Results

Gametogenesis dynamics

The histological sections corroborated that oocytes and spermatid cysts never co-occurred in the same individuals (i.e., gonochorism). Oocytes consistently showed intense affinity for the stains (Fig. 1b–f). The 2-year monitoring (2003–2005) indicated that oogenesis extended for several

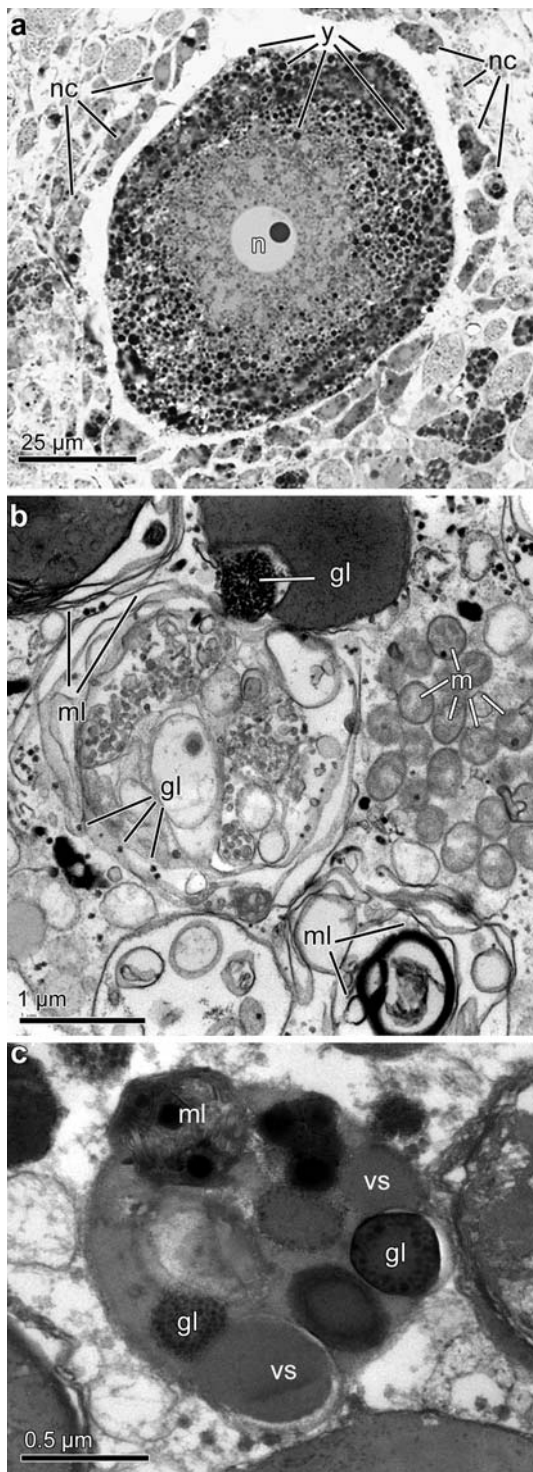


Fig. 3 Mid-size oocyte features. **a** General view of amoeboid, young oocyte containing abundant yolk inclusions (*y*) and surrounded by numerous nurse cells (*nc*). A non-vitellogenic area surrounds the nucleolate nucleus (*n*). **b** Immature yolk inclusions still showing patent multi-lamellar (*ml*) substructures and groups of glycogen granules (*gl*). There are adjacent clusters of small mitochondria (*m*). **c** A late-stage yolk body showing a more homogeneous substructure, in which glycogen (*gl*), vesicular (*vs*) and multi-lamellar (*ml*) components are little distinguishable

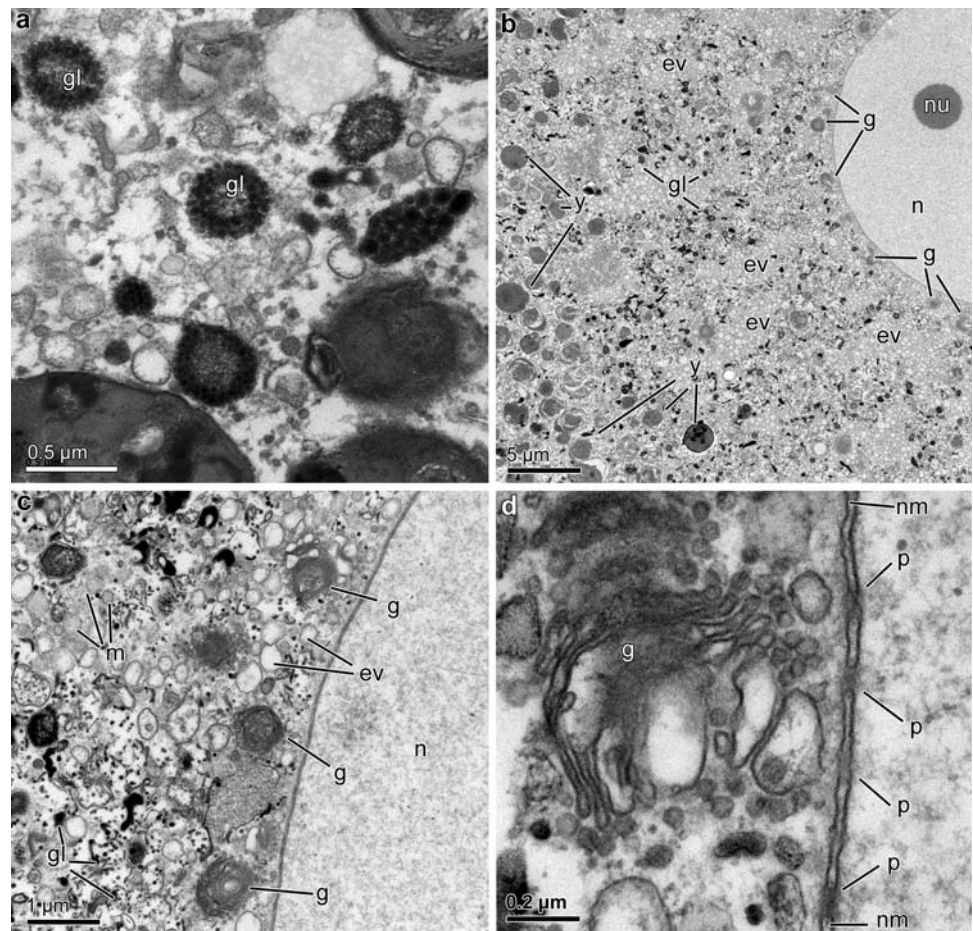
months each year, with some inter-annual variability (Fig. 2a). During 2004, oocytes were first detected in the sponge tissue in May, coincidentally with the spring water warming, and they were visible until late November (Fig. 2a). In contrast, although oocytes were also released in late November in 2005, the first oocytes were not detected until August that year. At the beginning of oogenesis small oocytes occurred sparsely scattered through the mesohyl (Fig. 1b), while sections taken towards the end of oogenesis showed large aggregated oocytes, usually below the endopinacoderm of exhalant canals (Fig. 1c). In November 2005 and 2006, we obtained ample evidence of large oocytes entering the excurrent channels (Fig. 1g–i).

Average production (\pm SD) of mature oocytes per mm^3 of sponge tissue was estimated as 3.6 ± 2.4 in 2004 and 5.6 ± 4.2 in 2005 (Fig. 2a). Nevertheless, these mean values must be taken cautiously, as indicated by their associated large standard deviations. It is likely that migration and clumping of oocytes during the course of oogenesis led to the underestimation of mean densities because our periodical sampling was restricted to small tissue portions taken from relatively superficial areas in order not to compromise sponge health. Sections also revealed mean oocyte size to increase progressively at an approximately constant rate during oogenesis in both years (Fig. 2b). Nevertheless, mature oocytes in 2005 had a smaller average diameter than in 2004 (Fig. 2b). Smaller oocytes in 2005 could derive from the fact that oogenesis was shorter and the average number of produced oocytes higher (Fig. 2a).

We failed to detect spermatocysts by light microscopy in 2003, 2004, and 2005's samples, but identified them finally in 2006's sections (Fig. 1j–l). These cysts had also been highly elusive in previous research (Scalera-Liaci et al. 1973; Scalera-Liaci and Sciscioli 1975). Cysts were first noticed as small, loose cell groups with poor affinity for the stains (Fig. 1j). Spermatogenesis developed rapidly, with cysts occurring in the mesohyl of males no longer than about 2.5 weeks a year, usually in late November. The relationship between spermatogenesis and temperature was unclear. A summer maximum followed by a drastic temperature drop by mid November (Fig. 2a) could be speculated to trigger sperm production, if any relationship.

The combination of histological sampling and *in vivo* monitoring throughout 2006–2007 revealed that out of 26 tagged individuals, 4 contained no gametes, 15 had oocytes, and 7 others had spermatocysts and that such a sexual condition was maintained over the entire study period. Therefore, about 57.7% of individuals in the population should be expected to be females and 27% to be males, with a 2:1 female/male sex ratio. Two of the four sponges that never contained gametes were relatively small

Fig. 4 Mid-size oocyte features. **a** Glycogen (*gl*) organized in rosettes. **b–c** View of the cytoplasmic vicinity of the nucleolate (*nu*) nucleus (*n*), which virtually lacks yolk bodies (*y*), but contains many electron-clear vesicles (*ev*), glycogen granules (*gl*), mitochondria (*m*), and numerous units of the Golgi apparatus (*g*). **d** Detail of a Golgi apparatus unit (*g*) adjacent to the nuclear membrane (*nm*), which shows several pores (*p*) filled with migrating material, probably mRNA



(<60 cm³) and probably were sexually immature; the two others were relatively large (>280 cm³) and apparently healthy. Therefore, we cannot exclude the possibility that the latter ones were actually males in which we failed to identify the spermatid cysts.

Ultrastructure of oogenesis

We were unable to identify the origin of oogonia. The smallest recognizable female reproductive cells were 10 to 20 μm, relatively amoeboid oocytes (Fig. 1b, d). They initially occurred so sparsely scattered in the mesohyl (Fig. 1b) that we failed to retrieve them in ultra-thin TEM sections. For this reason, our ultrastructural description mostly focuses on mid-stage (50–150 μm) and late-stage oocytes (Fig. 1e–i). Mid-size oocytes were also somewhat amoeboid (Fig. 3a). They contained abundant, large electron-dense yolk inclusions, which were consistently membrane bound. At this stage, most yolk inclusions consisted of a complex combination of heterogeneous materials, often showing multi-membrane substructure and incorporating abundant glycogen granules (Fig. 3b). Only few yolk bodies showed the relatively homogeneous substructure that

characterized yolk in mature oocytes (Fig. 3c). Clusters of small mitochondria (Fig. 3b) and rosettes of glycogen granules (Fig. 4a) were common among the yolk bodies. The nucleolate nucleus was surrounded by a 20 μm-wide perinuclear region in which yolk bodies were absent (Fig. 4b–c). This perinuclear region contained multiple units of the Golgi apparatus, clusters of mitochondria, abundant small electron-translucent vesicles, and glycogen granules (Fig. 4b–d). The nuclear membrane of mid-size oocytes showed evident pores, through which unidentified material (probably mRNA) migrated (Fig. 4d).

Mid-size oocytes were usually surrounded by a lax cell layer consisting of nurse cells, specialized pocket cells (i.e., bacteriocytes, hosting enormous amounts of living bacteria), and, most peripherally, large spherulous cells (Fig. 5a, b). All those cells never formed a continuous follicle-like epithelium. Rather, they occurred as amoeboid cells moving around oocytes in the perioocyte space. Nurse cells actively participated in oocyte vitellogenesis, as revealed by a cytoplasm charged with phagocytosed bacteria and heterogeneous yolk granules identical to those also occurring in the oocytes (Fig. 5c). Nurse cells often established intimate contact with oocytes, sometimes being deeply

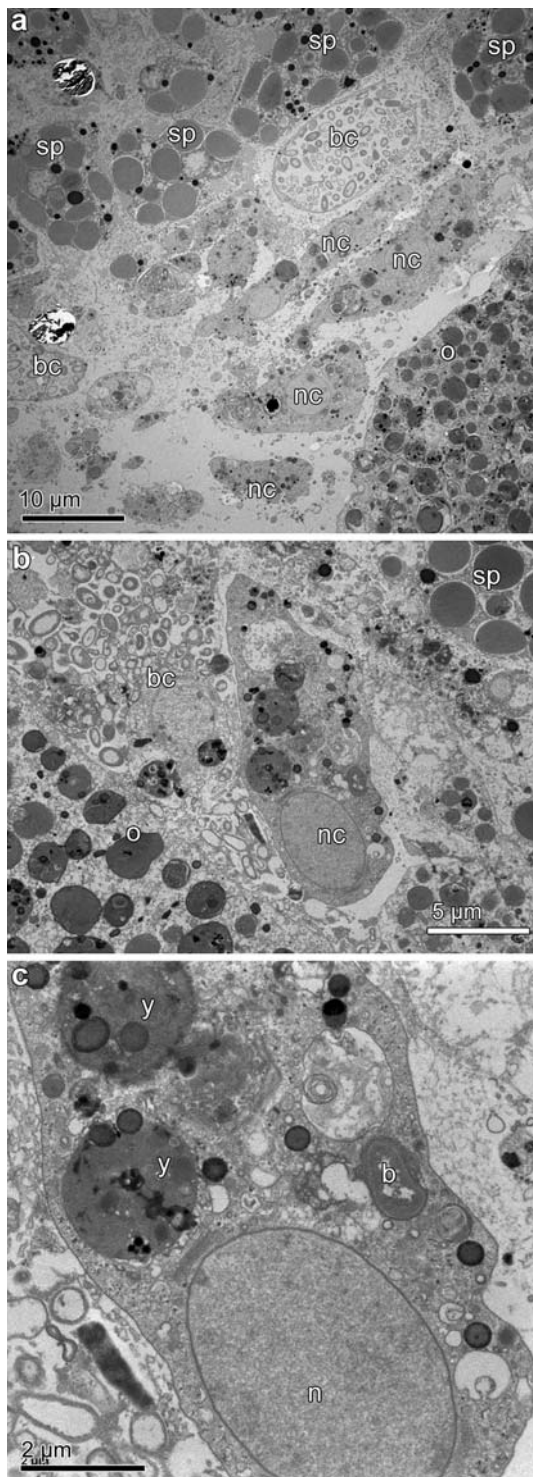


Fig. 5 Oocyte envelope. **a, b** Developing oocyte (*o*) surrounded by nurse cells (*nc*), bacteriocytes (*bc*) and, more peripherally, spherulous cells (*sp*). **c** Detail of the nurse cell in micrograph (**b**) showing part of the nucleus (*n*), an engulfed bacterium (*b*), and newly produced yolk bodies (*y*)

embraced by the oocyte membrane (Fig. 6a). Some narrow cytoplasmic bridges between nurse cells and the oocyte (Fig. 6b) were formed for probable transference of small

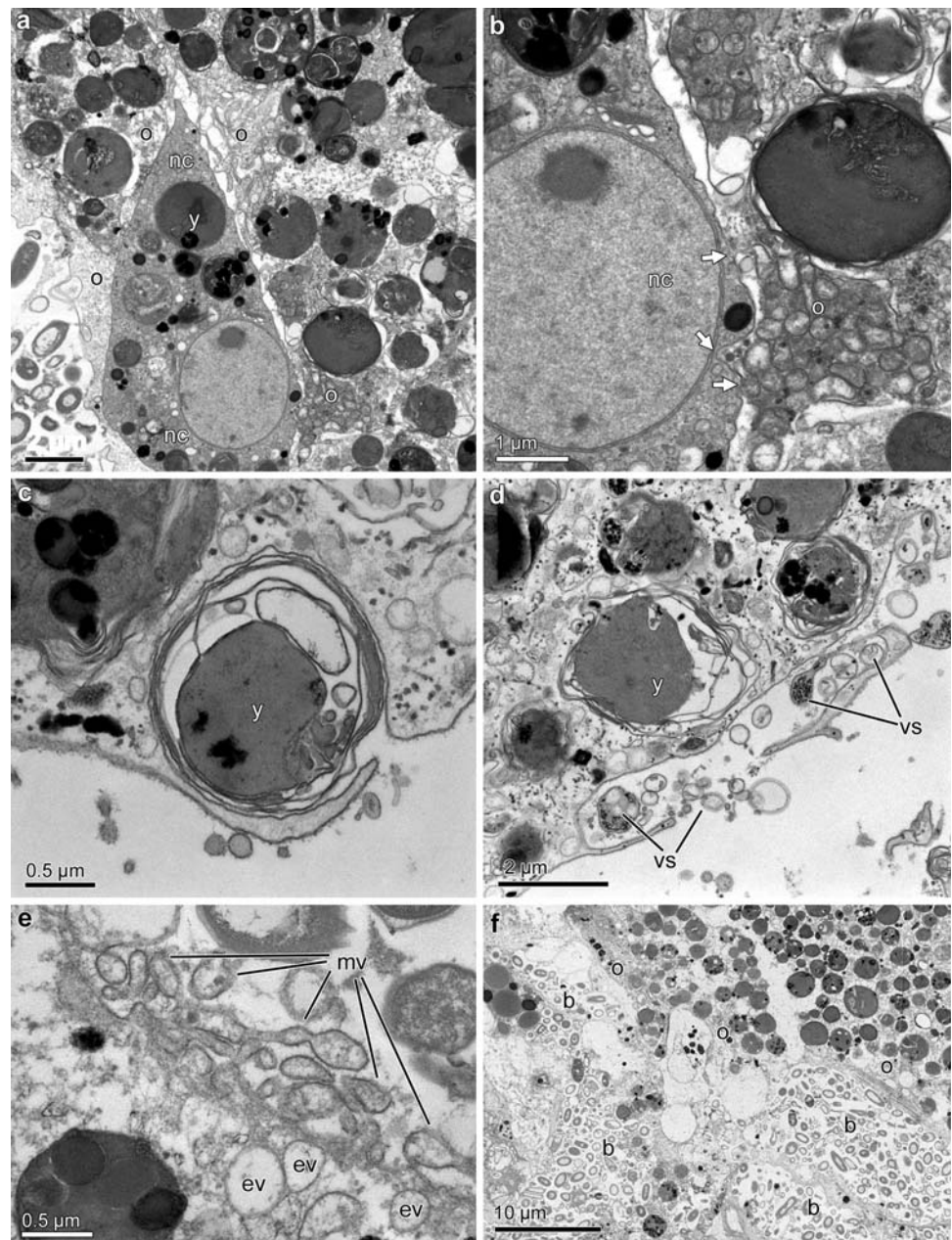
inclusions and yolk precursors. In addition, nurse cells exocytosed in the vicinity of the oocytes yolk bodies and large inclusions, which were subsequently engulfed by oocyte pseudopodia (Fig. 6c, d). Abundance of small electron-clear vesicles in the periphery of the oocytes suggests that they were also able to pinocytose soluble compounds (Fig. 6e). Bacteriocytes released abundant bacteria to the perioocyte mesohyl (Fig. 6f). We never obtained evidence of oocytes directly engulfing these freed bacteria, but they were engulfed by nurse cells (Fig. 5c). Groups of spherulous cells occurred peripherally to the nurse cells and bacteriocytes that surrounded the oocytes (Fig. 5a, b). Nevertheless, no obvious involvement of these spherulous cells in the oogenesis was realized.

Mature oocytes (200–250 µm) showed a cytological organization similar to that described for mid-size oocytes, but lacked the nucleolus. The perinuclear cytoplasm lacked yolk bodies (Fig. 7a), but contained many units of the Golgi apparatus, isolated round mitochondria, glycogen granules, free ribosomes, and electron-clear vesicles (Fig. 7b). The remaining cytoplasm was heavily charged with membrane bound, electron-dense yolk bodies of variable size (Fig. 7c). These yolk bodies were more homogeneous in content than those found in mid-size oocytes, though diverse components were still evident (Fig. 7d), some of them showing the para-crystalline substructure typical of proteinaceous materials (Fig. 7e). Unlike in mature oocytes of other demosponges, lipid droplets occurred at very low density. The most peripheral cytoplasm of the mature oocyte was characterized by many small, electron-clear vesicles (Fig. 7f) probably resulting from pinocytosis. The membrane of mature oocytes formed periodical stout microvilli and was enveloped by a 0.5-µm thick layer of mucus-like material (Fig. 7g).

Ultrastructure of spermatogenesis

Because spermatogenesis was relatively rapid, our TEM follow-up provided fragmentary information for some of the steps, which will require further research. At the onset of spermatogenesis i.e., about 2.5 weeks before spawning the choanocyte chambers started showing some enlarged choanocytes (Fig. 8a). These swollen choanocytes entered the mesohyl and formed large aggregates. At this stage, many choanocyte chambers were still functional in the adjacent tissue, so that the transdifferentiation process of choanocytes into spermatogonia only affected to either some cells in each chamber or few entire chambers. It was unclear whether or not the flagellum was disassembled during the transdifferentiation and additional observations would be required to corroborate this issue. Spermatogonia still contained many phagosomes and diverse inclusions similar to those characterizing the cytoplasm of the

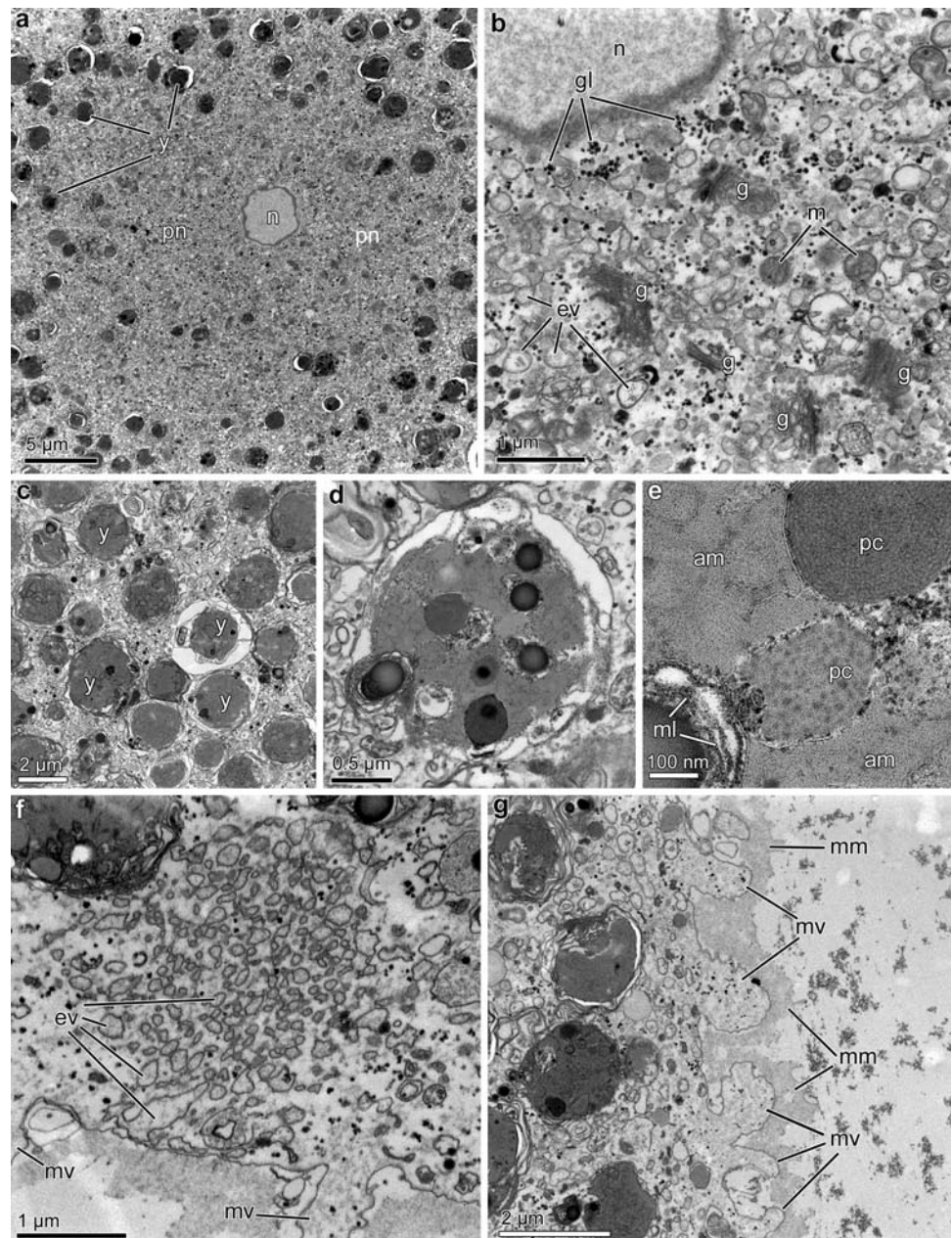
Fig. 6 Oocyte nourishment. **a** Nurse cell (*nc*) charged with yolk bodies (*y*) being deeply embraced by the oocyte (*o*). **b** Detail of nurse cell (*nc*) in (**a**), showing membrane areas (*arrows*) in close contact with the oocyte (*o*). **c, d** Details of oocytes engulfing yolk bodies (*y*) and other vesiculate materials (*vs*) released to the perioocytic space by the nurse cells. **e** Microvilli (*mv*) of the oocyte membrane with cytoplasmic production of electron-clear vesicles (*ev*) suggesting pinocytosis from the perioocytic space. **f** Abundant bacteria (**b**) released by bacteriocytes to the vicinity of oocytes (*o*)



choanocytes in the chambers (Fig. 8b). Primary spermatocytes formed large groups in the mesohyl, without being initially limited by any sort of follicle (Fig. 8c) They measured approximately 3 μm in the largest diameter, showed some typical synaptonemal complexes in their nucleus and were flagellated (Fig. 8d–f). No accessory centriole was noticed in the basal apparatus of the spermatocyte flagellum. Some of the cytoplasmic inclusions characterizing the cytoplasm of choanocytes and spermatogonia persisted in the cytoplasm of both primary and secondary spermatocytes (Fig. 8d–g). Secondary spermatocytes showed, in addition to remains of phagosomes, a nucleus with partially condensed chromatin, a relatively

large cytoplasm containing several small mitochondria (Fig. 8g), and a flagellum (not shown). As typical in animal spermatogenesis, cytoplasmic bridges connected the sister cells resulting from successive spermatogenic divisions (Fig. 8g). The spermatogenesis was highly synchronous at both the cyst level and the individual level. Mature spermatozoa were characterized by a round head containing a large nucleus, three large, round mitochondria, and up to 13 electron-dense proacrosomal vesicles, typically located at the cell (anterior) pole opposite to the flagellum insertion (Fig. 9a, b). Proacrosomal vesicles were membrane bound and contained granulo material (Fig. 9c). The condensed chromatin of the nucleus typically occupied the central

Fig. 7 Late-stage oocyte features. **a** Perinuclear area (*pn*) lacking yolk bodies (*y*) around the nucleus (*n*) of mature oocytes. **b** Detail of the perinuclear area, showing abundant glycogen (*gl*), mitochondria (*m*), and electron-clear vesicles (*ev*), as well as five units of the Golgi apparatus (*g*). **c** Detail of an intermediate cytoplasmic region heavily filled with membrane-bound yolk bodies (*y*). **d** Mature yolk body showing amalgamation of diverse compounds and materials. **e** Magnification of yolk body in Fig. 7 showing pseudo-crystalline (*pc*), amorphous (*am*), and multi-lamellar (*ml*) materials. **f** Detail of the peripheral cytoplasm showing microvilli (*mv*) and abundant small electron-clear vesicles (*ev*). **g** General view of the membrane of mature oocytes, which forms regular, stout microvilli (*mv*) and is covered by a layer of mucus-like material (*mm*)



region, leaving a peripheral, narrow band of uncondensed material (Fig. 9a, b). The basal apparatus of the flagellum consisted of a principal centriole (basal body) and a perpendicular accessory centriole (Fig. 10a). There were not other evident cytoskeletal components associated with the basal apparatus of the cilium.

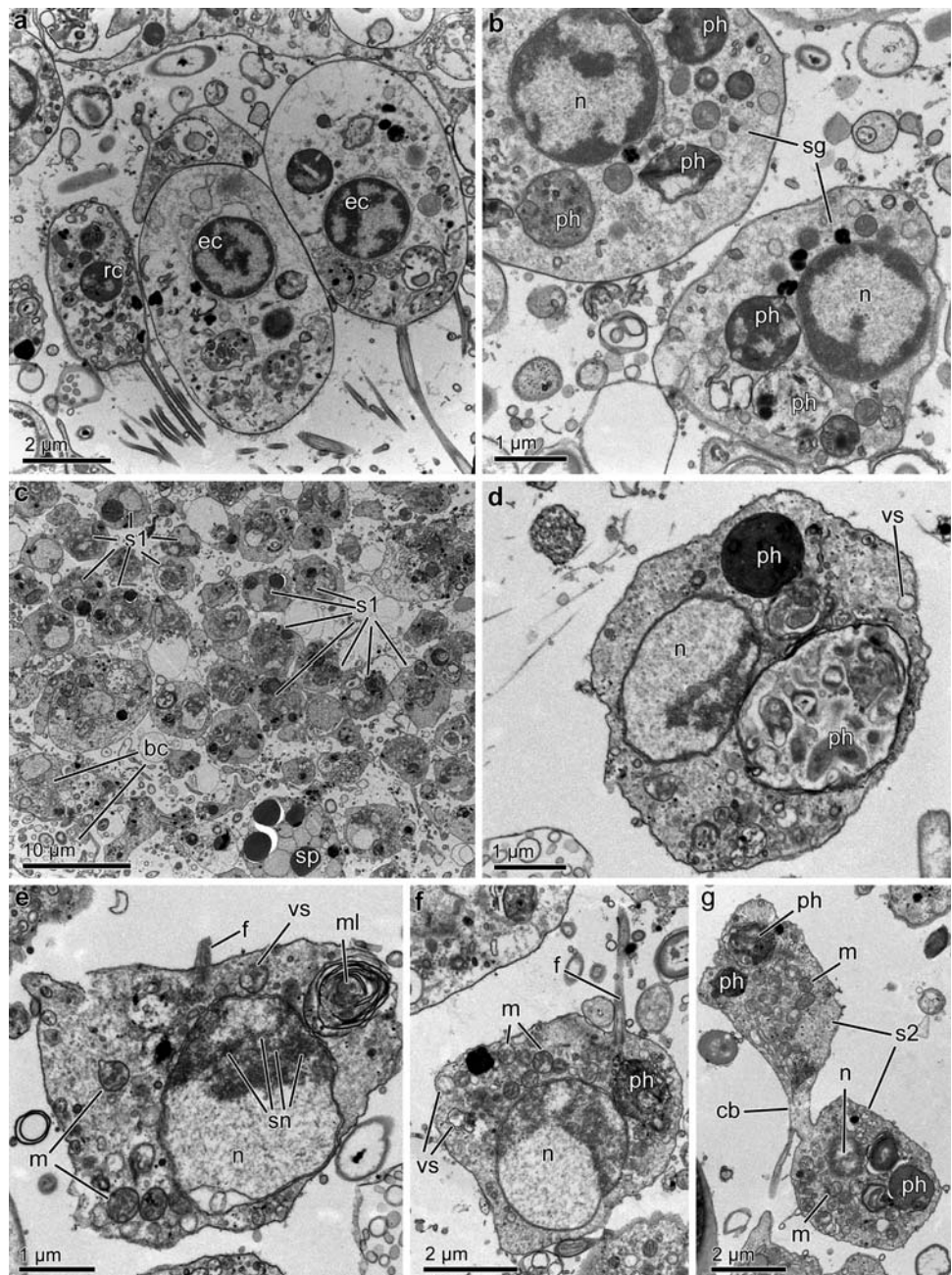
Spermatic cysts were limited by a continuous epithelium of follicular cells (Fig. 10a, b), which was in turn surrounded by a lax layer of large bacteriocytes charged with bacteria (Fig. 10a, b). Follicle cells were flat, pavement-like, thickened only at a central zone, in which the nucleus and abundant small electron-clear vesicles occurred (Fig. 10b, c). Contacts between adjacent follicle cells were

by either juxtaposition or simple interdigitations, with no obvious membrane specialization (Fig. 10d, e). After spawning, several types of mesohyl cells entered the cysts to engulf non-spawned spermatozoa, as recently detailed elsewhere (Riesgo et al. 2008).

Fertilization and embryo development

Spawning occurred in the morning of two consecutive days in December 2006 and a single day in November 2007. Detailed information on the biology of spawning is provided elsewhere (authors, in prep.). Upon release, eggs measured $259.6 \pm 19.7 \mu\text{m}$ on average ($n = 30$).

Fig. 8 Features of early spermatogenesis. **a** Regular choanocyte (*rc*) adjacent to choanocytes (*ec*) that are enlarging to become spermatogonia. **b** Spermatogonia (*sg*) showing a nucleus (*n*) with peripheral chromatin condensation and a cytoplasm containing inclusions and phagosomes (*ph*) that are characteristic of the choanocyte cytoplasm. **c** Aggregation of primary spermatocytes (*s1*) adjacent to bacteriocytes (*bc*) and spherulous cells (*sp*), but lacking a follicle. **d–f** Diverse sections of primary spermatocytes, showing the flagellum (*f*), the nucleus (*n*) with synaptonemal complexes (*sn*), and a cytoplasm containing diverse multi-lamellar (*ml*) and vesiculate inclusions (*vs*), phagosomes (*ph*), and several small mitochondria (*m*). **g** Sister secondary spermatocytes (*s2*) showing the cytoplasmic bridge (*cb*), the nucleus (*n*), many small mitochondria (*m*), and remains of phagosomes (*ph*)



They came out bearing two, 12–15 µm translucent polar bodies attached, which were filled with turgid vesicles (Fig. 11a–c).

Fertilization took place externally. By mixing collected male and female gametes, we performed *in vitro* fertilization in Petri dishes. About 6 h after fertilization, a membrane appeared externally to the mucous layer of eggs (Fig. 11c). The polar bodies remained attached to this fertilization membrane (Fig. 11c). Eggs started dividing in the laboratory about 10 h after spawning (Fig. 11d). The plane of the first embryonic division was perpendicular to a

diametrical axis arising from the position at which the polar bodies occurred (Fig. 11e, h; see Video 1, as Supplementary Material). Initial cleavage was nearly equal and total, and took place relatively slowly, with about a 4 h-period required for the two-cell stage to reach the four-cell stage and a similar additional period to complete the eight-cell stage (Fig. 11e–j; see Video 1, as Supplementary Material). Blastomeres proliferated so strongly packed to each other that became polyhedral, giving rise to a spherical stereoblastula (Fig. 12a–c). The thin mucous layer and the fertilization membrane, which showed completely different

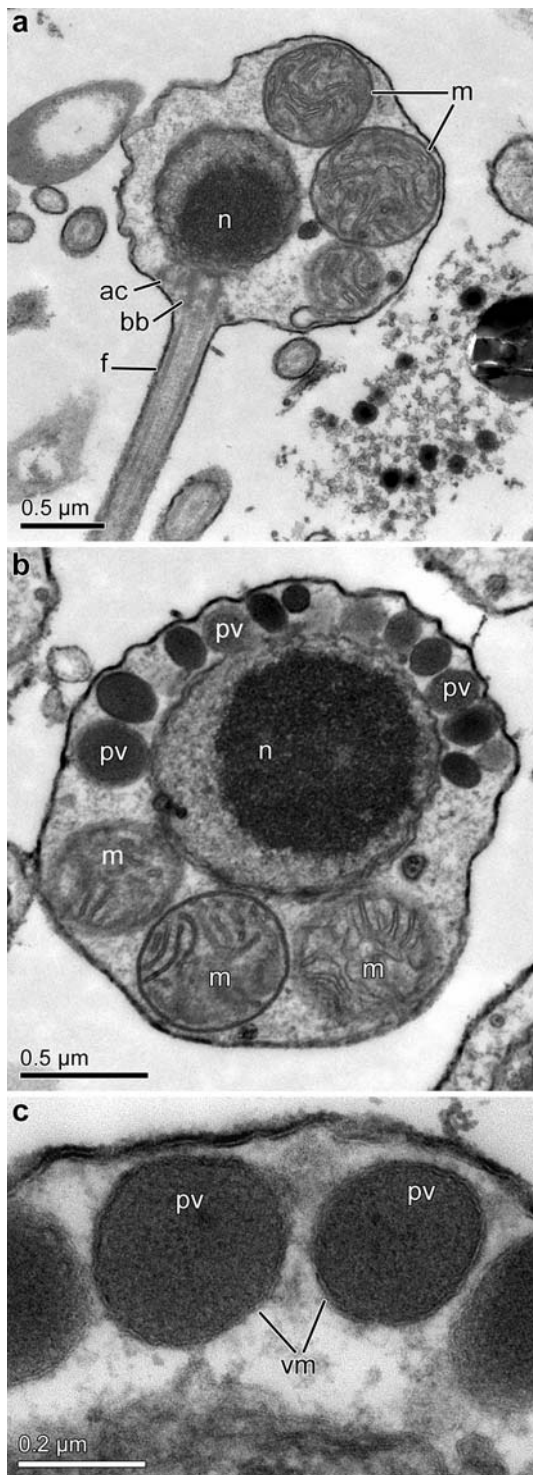


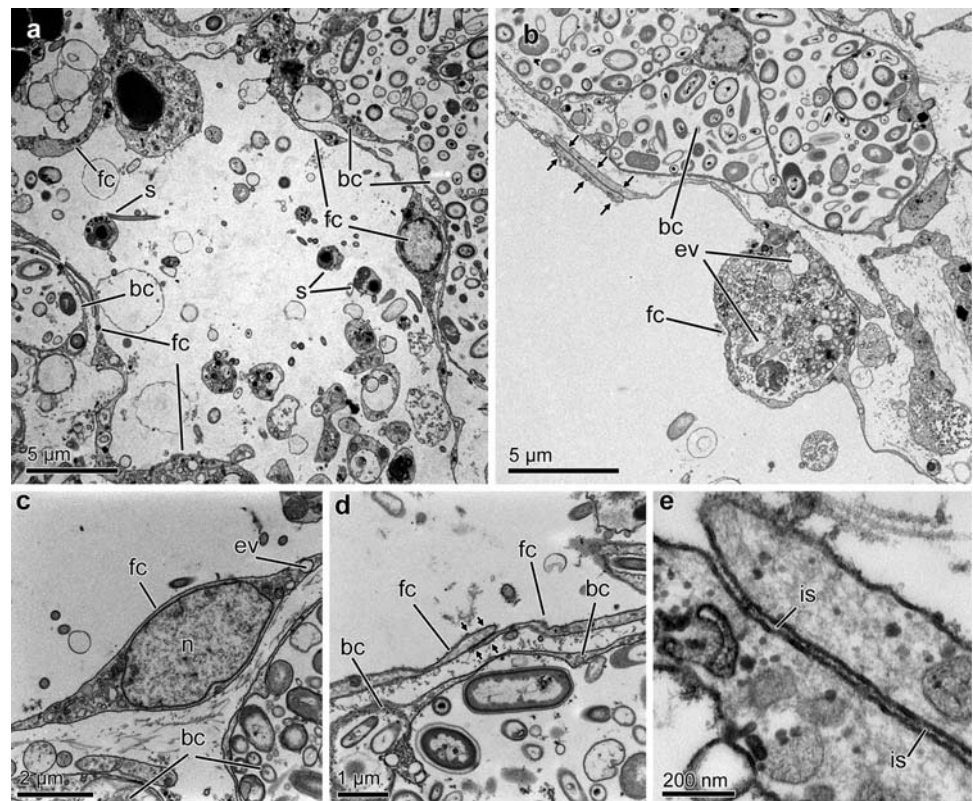
Fig. 9 Mature spermatozoa. **a** Longitudinal section of the spermatozoon showing the nucleus (*n*), three large mitochondria (*m*) and a flagellum (*f*) provided with a basal body (*bb*) and accessory centriole (*ac*). **b** Angling section of the spermatozoon showing a large battery of proacrosomal vesicles (*pv*), the nucleus (*n*) and large mitochondria (*m*). **c** Proacrosomal vesicles (*pv*) showing a finely granulated, electron-dense content bounded by a bi-layered membrane (*vm*)

substructural organization, were still enveloping the embryos during the earliest stages of cleavage (Fig. 12d–e).

Cilia appeared at about the 64-cell stage, but they started effectively beating only about 12 h later. Then, cell division accelerated and the fertilization membrane started dissolving. The first solid, multicellular spherical embryos with functional cilia were noticed about 36 h after fertilization (Fig. 11k; see Video 2, as Supplementary Material). These ciliated embryos correspond to the larval stage. At no time did they swim in the water of the Petri dishes. Rather, these 300–400- μm larvae were slow gliders that had the ability to remodel their body shape, producing transient lobules (Fig. 11i; see Videos 3–4, as Supplementary Material). Spontaneous changes in shape occurred at about 4 h intervals, perhaps stimulated by periodic waves of massive mitose of the larval cells (see Videos 3, as Supplementary Material). Larvae also produced transient lobules when disturbed (see Videos 4, as Supplementary Material). TEM observations revealed that the larval cells attained not much differentiation (Fig. 12c), irrespective of being at the body surface or at internal regions. The only difference was that peripheral cells were monociliated while internal ones were not (not shown). All larval cells showed a large nucleolate nucleus surrounded by many units of the Golgi apparatus (Fig. 13a–c). Their cytoplasm was heavily charged with yolk bodies, glycogen granules and electron-clear vesicles (Fig. 13a–c). Larval cells were tightly packed (Fig. 13a), only rarely allowing tiny intercellular spaces that contained diverse vesiculate material (Fig. 13d). Despite the intimate intercellular contacts, membrane specializations for special junctions were never noticed.

Larvae started attaching to the bottom of dishes about 2 weeks after spawning (Fig. 11m). Cilia were still visible for several hours in attaching larvae (Fig. 11n). Many multi-lobate larvae remained unattached on the bottom of the Petri dishes for about two additional weeks before successful attachment, indicating a potential large variability in the duration of embryonic development and larval life, at least in our laboratory conditions. Settlers initially produced thin, pointing protrusions (Fig. 11o). During attachment, settlers were able to fuse each other producing large chimeric aggregates (Fig. 11p). Juveniles developed obvious choanocyte chambers only after 1.5 months (not shown). After 3 months in the laboratory cultures, the young sponges had attained very little growth, although became more solid and non-translucent. The removal of small tissue pieces for spicule analysis under the light microscope corroborated that they have developed the small hastate oxeas characteristic of adult *P. ficiformis*, but somewhat thinner (not shown), as it would be expected for spicules developed under low availability of food and silicic acid.

Fig. 10 Spermatic cyst envelope. **a** Spawned spermatic cyst, in which only three spermatozoa (*s*) remain. Note the continuous envelope of follicle cells (*fc*) and the occurrence of peripheral bacteriocytes (*bc*). **b–c** Central region of follicle cells (*fc*) showing the nucleus (*n*) and small electron-clear vesicles (*ev*). Note the intercellular contact (*arrows*) between follicle cells (*fc*). Bacteriocytes (*bc*) occur peripherally to the follicle cells. **d** Contact (*arrows*) between the flat expansions of adjacent follicle cells (*fc*), which takes place by simple cell overlapping. Note the adjacent bacteriocyte (*bc*). **e** Magnification of contact between follicle cells showing no membrane specialization. Amorphous rather than spatially organized material occurs in the intercellular space (*is*)



Discussion

The reproductive cycle of *Petrosia ficiformis* was characterized by spawning in late autumn. In most sublittoral demosponges from the Atlantic-Mediterranean region reproduction occurs in the late spring or summer (e.g., Lévi 1956; Mercurio et al. 2007), probably stimulated by the previous seasonal temperature rising in spring. Nevertheless, a recent study has demonstrated that there is at least a set of oviparous species that release their gametes during the cold season (Riesgo and Maldonado 2008). *Petrosia ficiformis* is also to be added to that group. Similarly, declining temperatures have been suggested to stimulate the onset of reproduction of the Australian oviparous haplosclerid *Xestospongia bergquistia* and *X. testudinaria* in Autumn (Fromont and Bergquist 1994). In contrast, the Caribbean *Xestospongia muta* reproduces in spring (Ritson-Williams et al. 2005), although seasonal changes in seawater temperature are only subtle at those latitudes. The ecophysiological reasons for using different timing strategies remain unknown and could be of many types.

Our study of the *P. ficiformis* oogenesis corroborates previous findings by Lepore et al. (1995), but indicates that those authors described intermediate rather than mature oocytes. We also found that most individuals of the

population reproduce every year and that female/male ratios are about 2:1 or even closer to the parity. It is likely that the enormous difficulties to histologically identify males led to the “suspicious” 62:1 female/male ratio previously found in this sponge (Scalera-Liaci et al. 1973). We detected that oogenesis involved not only oocyte growth, but also a peculiar migration process. Most oocytes initially appeared in the innermost regions of the mesohyl but migrated progressively towards the vicinity of excurrent canals, where they aggregated to enter massively the canals immediately prior to spawning. According to our tissue sampling, duration of oogenesis was about 7 months in 2004, but only 4 months in 2005. A previous report by Scalera-Liaci et al. (1973), which was based on the very large numbers of individuals, reported a 8-month long oogenesis. Therefore, it is likely that oogenesis also extended in our sponges for 7–8 months in 2005, but we failed to detect the small stage oocytes characterizing the beginning of oogenesis. Shorter oogenesis (about 4–5 months) has been postulated for other viviparous haplosclerids in the genus *Xestospongia* (Fromont and Bergquist 1994). During 2005, oocytes reached a final size smaller than that in 2004 (Fig. 2), although were produced in higher numbers. Between-year variability in food availability and temperature may partially have accounted for those differences, but we cannot disregard that the

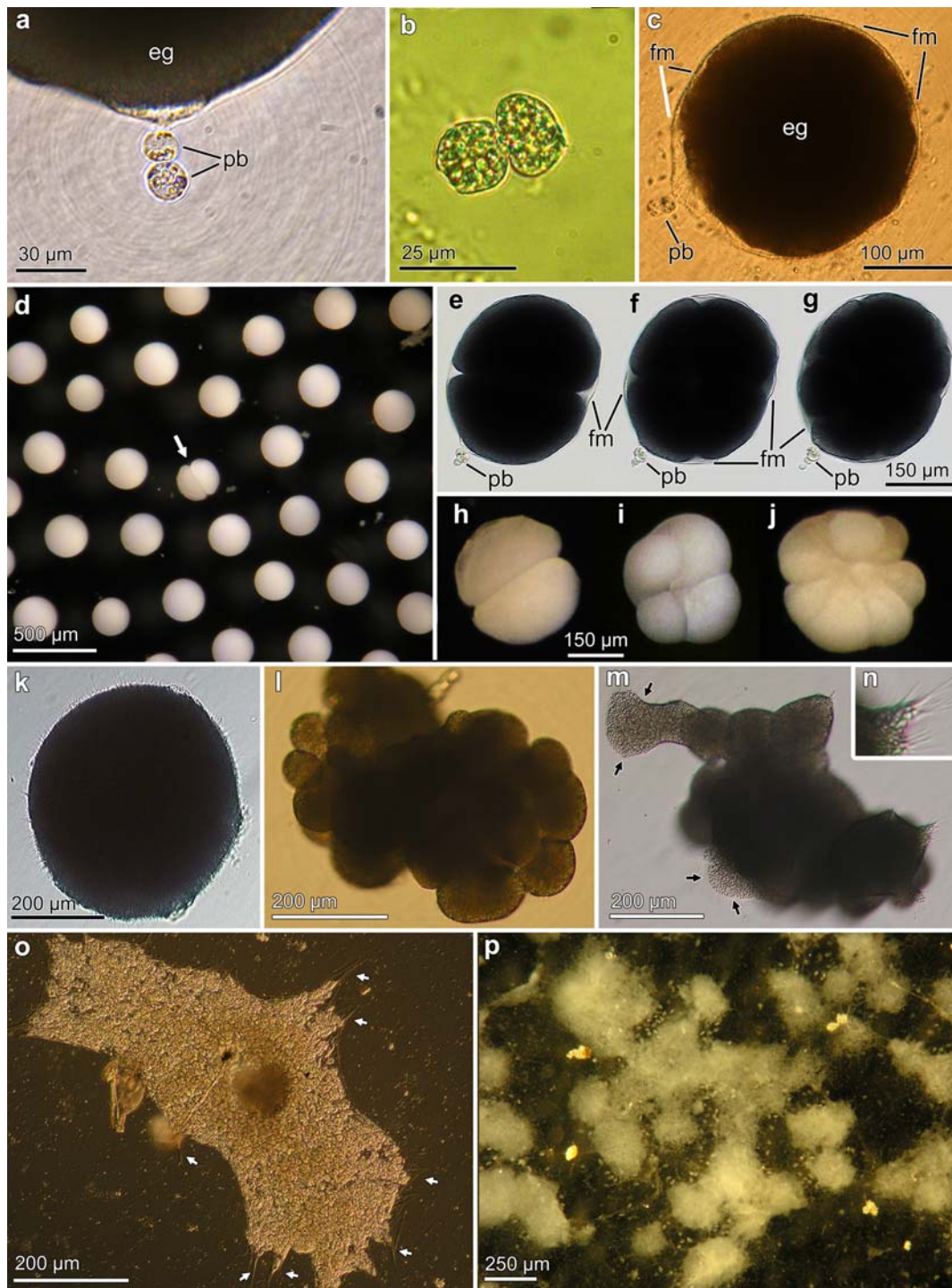


Fig. 11 In vivo observations on spawned eggs, embryos and juveniles. **a** Polar bodies (*pb*) attached to a released egg (*eg*). **b** Detail of polar bodies showing their many refringent vesicles. **c** Egg (*eg*) surrounded by a newly formed fertilization membrane (*fm*) bearing the polar bodies (*pb*) attached (*pb*). **d** A cleaved egg (*arrow*) surrounded by a majority of still undivided eggs. **e–g** Compound microscopy micrographs of a 2, 4, and 8-cell stages of a same embryo within a fertilization membrane (*fm*) that holds the polar bodies (*pb*). **h–j** Dissecting microscopy micrographs illustrating 2, 4, and 8-cell stages of embryos. **k–l** Views of the spherical multiciliated larva (**k**)

and its multilobate transitory morphology (**l**), respectively. The lobes do not correspond to a single cell, but are formed by dozens of them. **m** Multilobate settling larva, initiating attachment at several points (*arrows*). **n** Inset of Fig. 11m showing that cilia are still present at different regions of the larval body during the attachment process. **o** Early settler still lacking spicules and choanocytes chambers and characterized by thin, long protrusions (*arrows*). **p** Aggregate of 1.5-month-old settlers, which remain fused and have developed choanocytes chambers

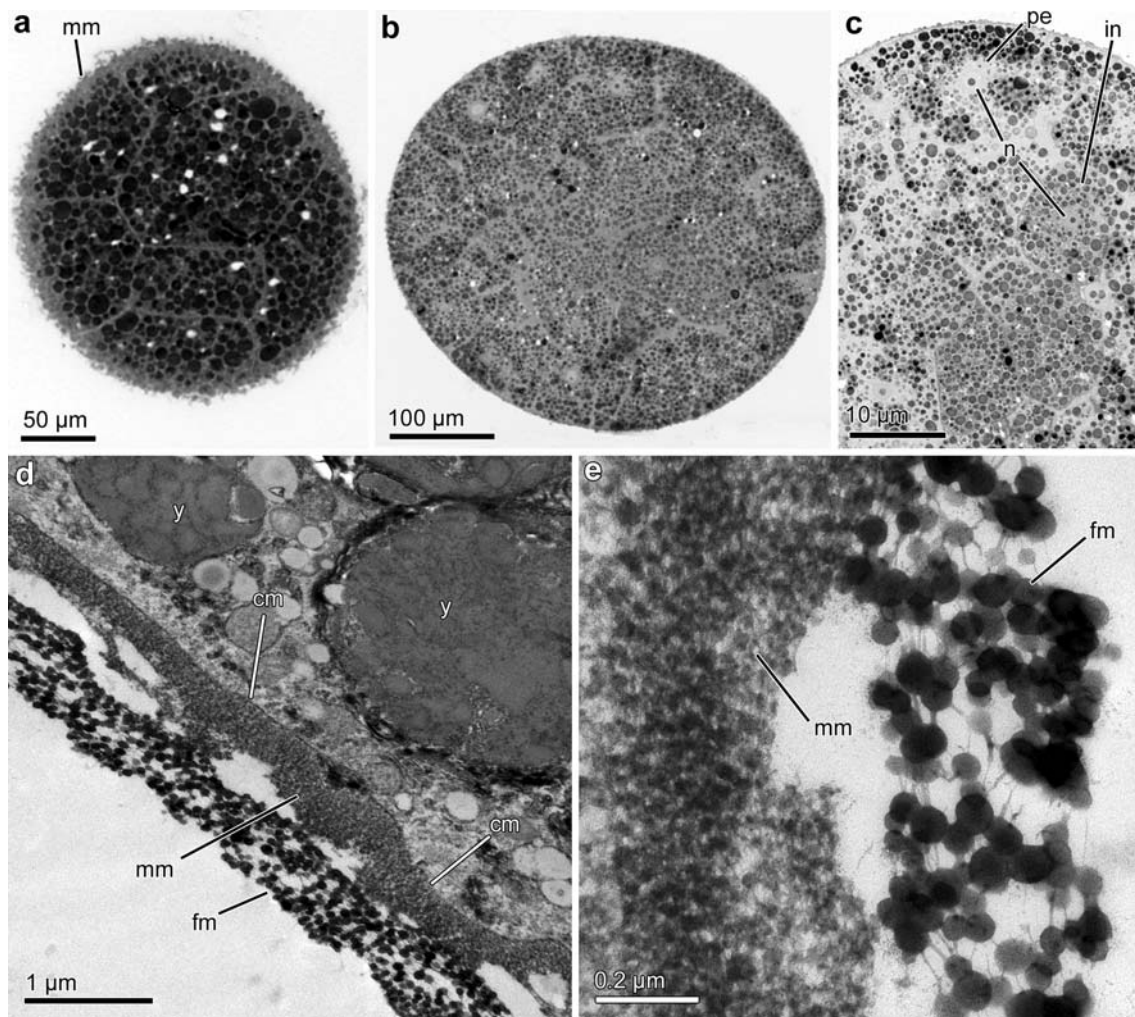


Fig. 12 Cytology of early embryos. **a, b** Section of an early stage and a late stage of the stereoblastula, showing relatively few, large, and polyhedral blastomeres. The mucous envelope (*mm*) is more developed in the early stage, while blastomeres are smaller, but more numerous in the late stage. **c** General view of internal (*in*) and

peripheral blastomeres (*pe*) in a late blastula. Nucleolate nuclei (*n*) are visible. **d** Peripheral blastomere showing yolk bodies (*y*), the cell membrane (*cm*), the mucous envelope (*mm*), and the fertilization membrane (*fm*). **e** Comparative view of the substructure of the mucous envelope (*mm*) and the fertilization membrane (*fm*)

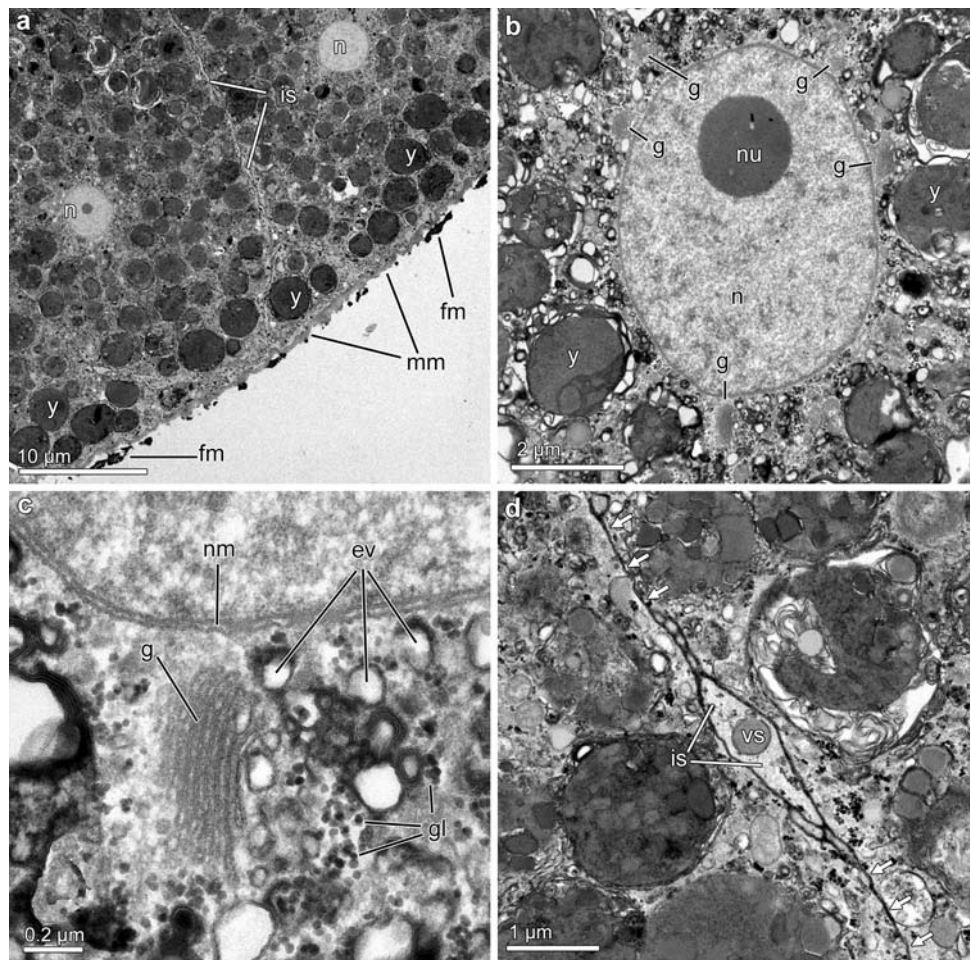
monthly tissue removal carried out during 2004 was also partially responsible for the 2005 pattern.

We found spermatogenesis to extend for about 2.5 weeks, in good agreement with the previous data by Scaleria-Liaci et al. (1973). Spermatogenesis shorter than a week has been postulated for several species of the genus *Xestospongia* (Fromont and Bergquist 1994). The spermatozoon of *P. ficiformis* was of the “primitive” type, similar in organization to that described in species from other demosponge groups, such as the viviparous *Aplysilla rosea* (Tuzet et al. 1970) and the oviparous *Suberites domuncula* (Diaz and Connes 1980). Because spermatogenesis was very rapid, we could not follow in detail the formation of proacrosomal vesicles from the Golgi apparatus. Nevertheless, they were virtually identical in

structure, size, and position to the proacrosomal vesicles known from the spermatozoon of many cnidarians, particularly corals. Another trait indicating that these structures were proacrosomal vesicles is that they first appeared during the spermatidogenesis, but not earlier in spermatogenesis, once the Golgi apparatus had been disassembled. Given the lack of information, a comparison between the ultrastructure of the spermatozoon of *P. ficiformis* and that of other viviparous haplosclerids is not possible yet.

Spawning in the studied population of *Petrosia ficiformis* took place during only 1 or 2 days a year, a restricted timing similar to that reported for several *Xestospongia* species (Fromont and Bergquist 1994; Ritson-Williams et al. 2005). External fertilization led to a slow cleavage

Fig. 13 Cytology of larvae **(a)** distal region of two peripheral larval cells. The nucleus (*n*) is nucleolate and the cytoplasm is filled with yolk granules (*y*). Intercellular spaces (*is*) are virtually non-existing. The mucous envelope (*mm*) is still visible, while most of the fertilization membrane (*fm*) has been dissolved. **b** Detail of the nucleolate (*nu*) nucleus (*n*) of a larval blastomere surrounded by several units of the Golgi apparatus (*g*) and yolk bodies (*y*). **c** Detail of a Golgi apparatus unit (*g*), the nuclear membrane (*nm*), in which pores are not visible, abundant glycogen granules (*gl*), and electron-clear vesicles (*ev*). **d** Detail of the contact region between two peripheral larval cells showing that the intercellular space (*is*) is collapsed in most areas (*arrows*) or allows tiny lacunae occupied by vesiculate material (*vs*)



that started after 6–10 h. In contrast, externally fertilized eggs of *Xestospongia* (Fromont and Bergquist 1994) and *Aplysina* (Maldonado 2009) are known to reach a 4 or 8-cell stages in only 4 h after spawning. The earliest cleavage stages occurred while embryos were still surrounded by the fertilization membrane and had the polar bodies attached. Interestingly, the plane of the first cleavage was perpendicular to a diametrical axis arising from the position of the polar bodies. This is exactly the same relative orientation reported by Tuzet (1970) during the cleavage of calcareous sponges and strengthens the view that sponge eggs may have a prefixed polarity.

The most outstanding finding of this study is probably the demonstration that the reproductive cycle of *Petrosia ficiformis* is characterized by the production of an entirely ciliated, solid larval stage. It is hard to decide whether this larva, which is characterized by a simple cytology of undifferentiated cells, may correspond to the ancestral condition of the parenchymella larval type or to a secondary simplification of such a type. It is worth noting that the extreme simplicity of this larva in terms of

cytology and behavior strongly contrasts with the features of the parenchymella larva of viviparous haplosclerids, which is one of the most sophisticated types in Porifera (Maldonado 2006). We are also confident that the fact that embryos were reared in vitro is not responsible for the described larval features. Embryos of 2 other oviparous species were reared by us in the laboratory during 2007 and 2008 (i.e., *Cliona viridis*: Maldonado and Riesgo 2008b; *Aplysina aerophoba*: Maldonado 2009). Unlike in *P. ficiformis*, the embryos of those other sponges developed into conventional swimming larvae in the laboratory. Furthermore, we obtained identical non-swimming larvae for *P. ficiformis* in two consecutive years (one of them is not reported in this manuscript). That the larva of *P. ficiformis* is not swimming is not unique feature in Porifera. The unciliated hoplitomella larva of genera such as *Thoosa* and *Alectona* is a heavy ball incorporating spicules and lacking cilia, and it does not swim. However, that larva is able to remain suspended in the plankton for dispersal during long periods (Maldonado and Bergquist 2002). Likewise, the ciliated

clavblastula larva of several species does not swim but only glides on the bottom (Maldonado and Bergquist 2002). The larva of *P. ficiformis* has limited abilities for both swimming and gliding. The ciliary beating probably enable this larva only to remain suspended in the plankton, while the slow development rates ensure at least 2 weeks of dispersal by turbulences, currents and waves. It is noteworthy that spawning days were characterized by moderate surge anticipating stormy conditions in both years. Given the limited ability for swimming and the absence of larval responses to light and other stimuli, the clear abundance of adults in shaded overhangs, walls and crevices must be explained by either preferential passive delivery of larvae to these microhabitats or enhanced survival of random settlers in them.

It is noteworthy that, despite the fact that the adults of *P. ficiformis* consistently harbor different types of symbiotic bacteria and cyanobacteria, these microbes were not found in mature oocytes, spermatozoa or embryos. Therefore, although the microbial symbionts of this sponge were initially suspected to be vertically transferred (Scalera-Liaci et al. 1973), our results are congruent with those by Lepore et al. (1995) and allow us to definitively conclude that microbes must be acquired from the ambient water by each new generation of juvenile sponges. This may also be the reason why most bacteria in the adult sponge remain within special bacteriocytes, as recently suggested in a more specific study on intergenerational transmission of microbial symbionts (Maldonado 2007).

It is difficult to assess the phylogenetic value of the features herein reported for *P. ficiformis* because the reproductive information available for oviparous haplosclerids is very scarce. The recent proposal that *Petrosia* and *Xestospongia* are not phylogenetically related but belonging to different subclades of Haplosclerida in which oviparism was acquired independently can be neither conclusively validated nor refuted from our results. Nevertheless, some interesting reproductive differences between both genera have been realized. *Petrosia* had longer gametogenesis, produced twice larger eggs that were spawned in isolation (not within sinking, sticky mucous threads), formed a fertilization membrane, and had slower embryonic development leading to a subspherical to multilobate, gliding larva somewhat different from the prolate (168–90 µm) larva reported for *Xestospongia* (Fromont and Bergquist 1994). Further reproductive studies on oviparous haplosclerids are urgently required to clarify the recently sparked debate on the monophyly of oviparity in the group, and for a more complete understanding of population dynamics and life histories to facilitate future actions on species conservation and management.

Acknowledgments The authors thank Alba Canyelles, Laura Núñez, Guillem Roca, and Sergio Taboada for help in fieldwork and Almudena García (Microscopy Service, UB) for help with TEM sample processing. We also thank Francesc Gómez for help with video processing. This study was funded by 2 grants of the Spanish Government (CTM2005-05366/MAR and BFU2008-00227/BMC).

References

- Barea-Azcón JM, Ballesteros-Duperón E, Moreno D (2008) Libro Rojo de los Invertebrados de Andalucía: Tomo IV. Junta de Andalucía, Sevilla
- Cerrano C, Magnino G, Sarà A et al (2001) Necrosis in a population of *Petrosia ficiformis* (Porifera, Demospongiae) in relation with environmental stress. *Ital J Zool* 68:131–136
- Diaz JP, Connes R (1980) Étude ultrastructurale de la spermatogénèse d'une Démosponge. *Biol Cell* 38:225–230
- Elvin DW (1976) Seasonal growth and reproduction of an intertidal sponge, *Haliclona permollis* (Bowerbank). *Biol Bull* 151:108
- Ferretti C, Marengo B, De Ciucis C et al (2007) Effects of *Agelas oroides* and *Petrosia ficiformis* crude extracts on human neuroblastoma cell survival. *Int J Oncol* 30:161–169
- Fromont J, Bergquist PR (1994) Reproductive biology of three sponge species of the genus *Xestospongia* (Porifera: Demospongiae: Petrosiida) from the Great Barrier Reef. *Coral Reefs* 13:119–126
- Lepore E, Sciscioli M, Gherardi M et al (1995) The ultrastructure of the mature oocyte and the nurse cells of the Ceractinomorpha *Petrosia ficiformis*. *Cah Biol Mar* 36:1520
- Lévi C (1956) Étude de *Halisarca* de Roscoff. *Embryologie et systématique des Demosponges*. *Arch Zool Exp Gén* 93:1–181
- Maldonado M (2006) The ecology of the sponge larva. *Can J Zool* 84:175–194
- Maldonado M (2007) Intergenerational transmission of symbiotic bacteria in oviparous and viviparous demosponges, with emphasis on intracytoplasmically compartmented bacterial types. *J Mar Biol Assoc UK* 87:1701–1713
- Maldonado M (2009) Embryonic development of verongid demosponges supports independent acquisition of spongin skeletons as alternative to the siliceous skeleton of sponges. *Biol J Linn Soc* 97:427–447
- Maldonado M, Bergquist PR (2002) Phylum Porifera. In: Young CM, Sewell MA, Rice ME (eds) *Atlas of marine invertebrate larvae*. Academic Press, San Diego, pp 21–50
- Maldonado M, Riesgo A (2008a) Reproductive output in a Mediterranean population of the homosclerophorid *Corticium candellabrum* (Porifera, Demospongiae), with notes on the ultrastructure and behavior of the larva. *Mar Ecol Evol Persp* 29:298–316
- Maldonado M, Riesgo A (2008b) Reproduction in the phylum Porifera: a synoptic overview. *Treb Soc Cat Biol* 59:29–49
- Maldonado M, Carmona MC, Velásquez Z et al (2005) Siliceous sponges as a silicon sink: an overlooked aspect of the benthopelagic coupling in the marine silicon cycle. *Limnol Oceanogr* 50:799–809
- Mercurio M, Corriero G, Gaino E (2007) A 3-year study of sexual reproduction in *Geodia cydonium* (Jameson 1811) (Porifera, Demospongiae) from a semi-enclosed Mediterranean bay. *Mar Biol* 151:1491–1500
- Poiret JLM (1789) *Voyage en Barbarie, ou lettres écrites de l'ancienne Numidie pendant les années 1785 & 1786, sur la religion, les coutumes & les mœurs des maures & des arabes-bédouins; avec un essai sur l'histoire naturelle de ce pays*. Deuxième Partie, Paris

- Redmond NE, McCormack GP (2008) Large expansion segments in 18S rDNA support a new sponge clade (Class Demospongiae, Order Haplosclerida). *Mol Phylogenet Evol* 47:1090–1099
- Redmond NE, van Soest RMW, Kelly M et al (2007) Reassessment of the classification of the Order Haplosclerida (Class Demospongiae, Phylum Porifera) using 18S rRNA gene sequence data. *Mol Phylogenet Evol* 43:344–352
- Regoli F, Cerrano C, Chierici E et al (2004) Seasonal variability of prooxidant pressure and antioxidant adaptation to symbiosis in the Mediterranean *Petrosia ficiformis*. *Mar Ecol Prog Ser* 275:129–137
- Riesgo A, Maldonado M (2008) Differences in reproductive timing between sponges sharing habitat and thermal regime. *Invertebr Biol* 127(4):357–367
- Riesgo A, Maldonado M, Durfort M (2007) Dynamics of gametogenesis, embryogenesis, and larval release in a Mediterranean homosclerophorid demosponge. *Mar Fresh Res* 58:398–417
- Riesgo A, Maldonado M, Durfort M (2008) Occurrence of somatic cells within the spermatocysts of demosponges: a discussion of their role. *Tissue Cell* 40(5):387–396
- Ritson-Williams R, Becerro MA, Paul VP (2005) Spawning of the giant barrel sponge *Xestospongia muta* in Belize. *Coral Reefs* 24:160
- Scalera-Liaci L, Sciscioli M (1975) Sexual cycles of some marine Porifera. *European Marine Biology Symposium Acts Suppl. Pubblicazioni della Stazione Zoologica di Napoli*, pp 307–316
- Scalera-Liaci L, Sciscioli M, Matarrese A (1973) Raffronto tra il comportamento sessuale di alcune Ceractinomorpha. *Riv Biol* 66:135–162
- Tuzet O (1970) La polarité de l'oeuf et la symétrie de la larve des éponges calcaires. *Symp Zool Soc London* 25:437–448
- Tuzet O, Garrone R, Pavans de Ceccatty M (1970) Observations ultrastructurales sur la spermatogenèse chez la Démospone *Aplysilla rosea* Schulze (Dendroceratide): Une métaplasie exemplaire. *Ann Sci Nat Zoologie 12eme Série*:27–50